# Human Intratumoral NKp46+ Natural Killer Cells are Spatially Distanced from T and MHC-I+ Cells with Prognostic Implications in Soft Tissue Sarcoma

Sylvia M. Cruz[1], Cyrus J. Sholevar[1], Sean J. Judge[2], Morgan A. Darrow[3], Khurshid R. Iranpur[1], Lauren E. Farley[1], Marshall Lammers[1], Aryana M. Razmara[1], Cordelia Dunai[4], Alicia A. Gingrich[5], Julia Persky[1], Hidetoshi Mori[6], Steve W. Thorpe[7], Arta M. Monjazeb[8], William J. Murphy[4], Robert J. Canter[1]

[1]Division of Surgical Oncology, Department of Surgery; [2]Department of Surgery, Memorial Sloan Kettering Cancer Center, New York, NY; [3]Department of Pathology and Laboratory Medicine; [4]Department of Dermatology; [5]Department of Surgical Oncology, MD Anderson Cancer Center, Houston, TX; [6]Center for Immunology and Infectious Diseases, University of California Davis; [8]Department of Radiation Oncology; [7]Division of Musculoskeletal Oncology, Department of Orthopedic Surgery.

This work was supported in part by National Institutes of Health/National Cancer Institute grant T32CA251007 and a generous grant from the UC Davis Comprehensive Cancer Center

## Abstract

Soft tissue sarcomas (STS) are heterogenous malignancies with an unmet need for novel immunotherapies. Tumor infiltrating lymphocytes (TILs) have previously been linked with favorable outcomes in STS patients, though the contribution of natural killer (NK) cell subsets, including NKp46 and CD56$^{bright/dim}$, has yet to be investigated in detail. Despite the known role of MHC-I on immunoregulation of NK and T cells, limited data exist characterizing the spatial relationship of NK cells to MHC-I$^{+/-}$ cells and T cells in the STS tumor microenvironment (TME). Using STS specimens from 130 patients, we evaluated intratumoral NK cell subsets by immunohistochemistry (IHC), flow cytometry, and immunofluorescence (IF) to assess their impact on overall survival (OS) and metastasis-free survival (MFS). We also assessed the spatial localization of NK and T cells by multiplex IF in the TME, specifically analyzing the effects of MHC-I expression status on NK and T cell clustering. High intratumoral NKp46 expression was associated with improved OS by IHC (P=0.04) and IF (P=0.02). CD56$^{dim}$ NK cells were associated with a survival benefit (P=0.05), while higher infiltrates of CD56$^{bright}$ NK cells predicted worse prognosis (P=0.05). CD3$^{-}$CD56$^{+}$ NK cells demonstrated a significant inverse relationship with CD3$^{+}$ T cells by both flow cytometry and IF. Spatial analyses showed NK cells preferentially clustering close to other NK cells with sparse CD3$^{+}$ T and CD8$^{+}$ T cells in range. (P<0.0001). Additionally, CD3$^{+}$ T and CD8$^{+}$ T cells showed significantly greater co-localization with MHC-I$^{+}$ cells, compared to NKp46+ NK cells (P<0.0001). Intratumoral NK cell subsets, including NKp46$^{+}$ and CD56$^{bright/dim}$ NK cells, are prognostic in STS and localize closer to MHC-I$^{-}$ cells than they do to T cells or MHC-I$^{+}$ cells. Although both NK and T cells are associated with improved survival in STS, their differential distribution in the TME based on MHC-I expression status reinforces inherent opposite but interconnected roles for these cells in anti-tumor surveillance.

| Characteristic | | IHC (N=100) | Flow Cytometry (N=46) | Multiplex IF (N=71) |
|---|---|---|---|---|
| Sex | Female | 41 (41%) | 19 (41%) | 32 (45%) |
| Age at diagnosis | | 59.8 ± 18.2 | 62.2 ± 15.3 | 61.8 ± 17.2 |
| Tumor size (cm) | | 13.2 ± 8.3 | 13.4 ± 9.6 | 13.9 ± 9.9 |
| Tumor site | Extremity | 67 (67%) | 25 (54%) | 41 (58%) |
| Histology | Undifferentiated pleomorphic sarcoma | 30 (30%) | 9 (20%) | 16 (23%) |
| | Liposarcoma | 22 (22%) | 11 (24%) | 20 (28%) |
| | Myxofibrosarcoma | 18 (18%) | 11 (24%) | 16 (23%) |
| Neoadjuvant therapy | Radiation | 53 (53%) | 28 (61%) | 40 (56%) |
| | Upfront surgery | 29 (29%) | 8 (17%) | 19 (27%) |
| | Chemoradiation | 13 (13%) | 10 (22%) | 9 (13%) |
| | Chemotherapy | 5 (5%) | 0 (0%) | 3 (4%) |

**Table 1.** Patient demographic and clinicopathologic characteristics of 130 total STS patients stratified by method of analysis.

A

| | N=130 | % |
|---|---|---|
| Progression to metastases | 61 | 47% |
| Alive without evidence of disease | 50 | 38% |
| Alive with disease | 40 | 31% |
| Died | 40 | 31% |

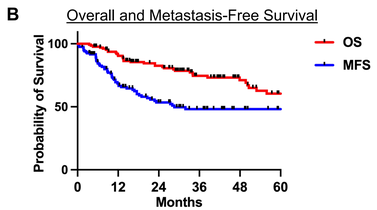


**Figure 1.** (A) Oncologic outcomes and (B) 5-year overall and metastasis-free survival of 130 STS patients.

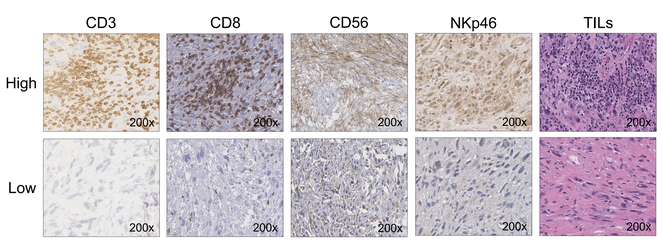


**Figure 2.** Representative immunohistochemical photomicrographs of high and low staining for CD3, CD8, CD56, NKp46, and representative H&E staining for tumor infiltrating lymphocytes (TILs).

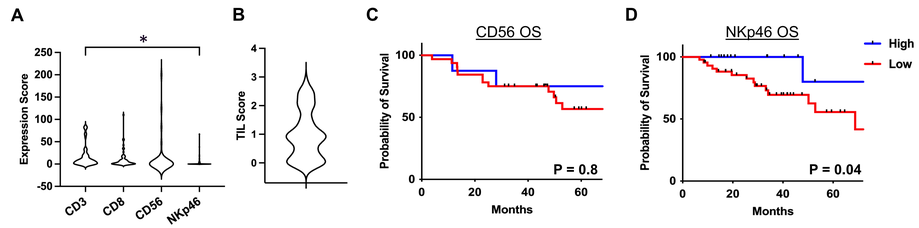


**Figure 3.** (A) Distribution of mean expression scores for CD3, CD8, CD56, and NKp46, and (B) mean TIL scores showing low scores on average with broad ranges. (C) CD56 stratified by median expression score does not show an association with OS by Kaplan-Meier analysis. (D) Kaplan-Meier analysis of OS stratified by median NKp46 showing superior OS in patients with high NKp46 expression scores (P=0.04).

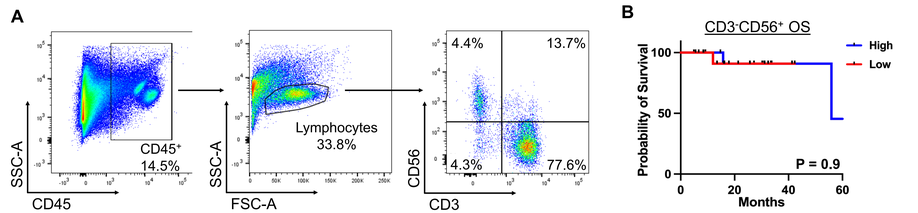


**Figure 4.** (A) Representative flow cytometry showing gating strategy for identification of NK and T cells in STS TME. (B) Kaplan-Meier analysis of OS stratified by median CD3$^{-}$CD56$^{+}$ frequencies showing no difference in survival outcomes.

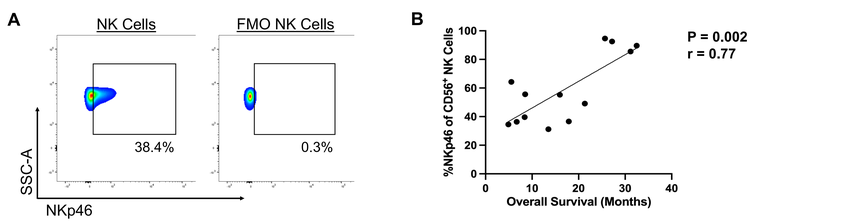


**Figure 5.** (A) Representative flow cytometry gating showing expression of NKp46 in the CD56$^{+}$ NK cell population (left) and control FMO staining (right). (B) Strong positive correlation of %NKp46 of CD56$^{+}$ NK cells with OS (P=0.002, r=0.77).

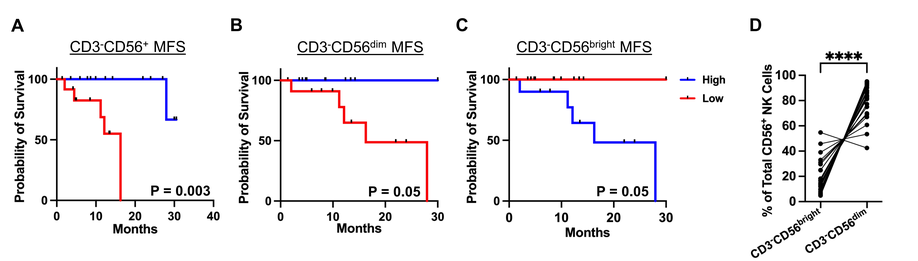


**Figure 6.** (A) Kaplan-Meier analysis of MFS stratified by median CD3$^{-}$CD56$^{+}$ frequencies, showing MFS benefit with high CD3$^{-}$CD56$^{+}$ frequencies (P=0.003). (B-C) Kaplan-Meier analysis of MFS stratified by median (B) CD3$^{-}$CD56$^{dim}$ and (C) CD3$^{-}$CD56$^{bright}$ frequencies, showing improved outcomes with high CD3$^{-}$CD56$^{dim}$ and worse outcomes with high CD3$^{-}$CD56$^{bright}$, respectively. (D) Paired analysis of CD3$^{-}$CD56$^{bright}$ and CD3$^{-}$CD56$^{dim}$ intratumoral NK cells as a percent of total CD56$^{+}$ cells, with significantly higher frequencies of intratumoral CD3$^{-}$CD56$^{dim}$ NK cells (P<0.0001). ****, P<0.0001.

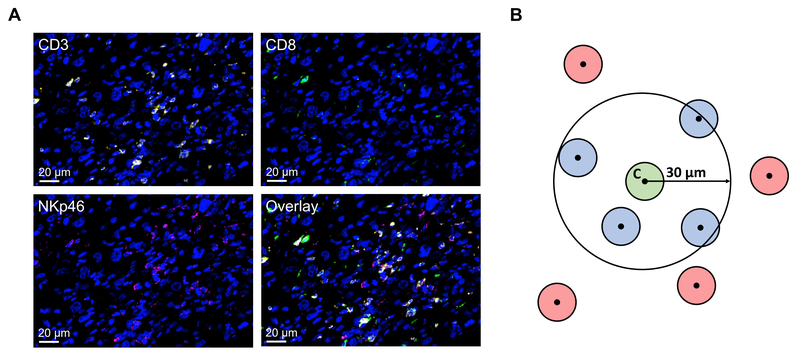


**Figure 7.** (A) Representative immunofluorescence photomicrographs of CD3, CD8, NKp46, and overlay of the three markers in soft tissue sarcoma tumor microenvironment. (B) Graphic illustrating spatial analysis of target cells (blue) within 30μm radius of a center cell (green). Cells out of radius (red) were not considered in-range.

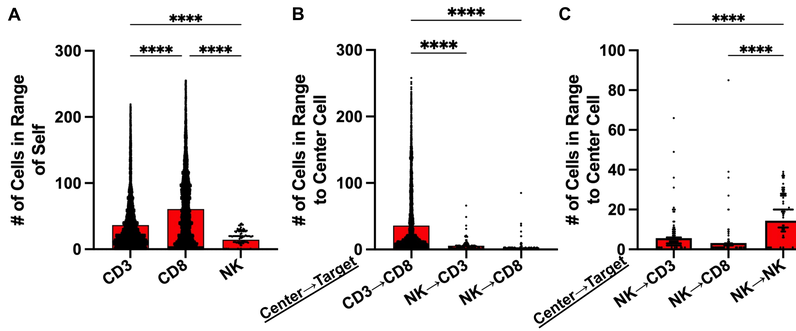


**Figure 8.** (A) Number of CD3$^{+}$ T, CD8$^{+}$ T, and NKp46$^{+}$ NK cells within 30μm radius of index effector cell of interest. (B) Number of CD3$^{+}$ T, CD8$^{+}$ T, and NKp46$^{+}$ NK cells in 30μm radius to center cells (CD3$^{+}$ T and NKp46$^{+}$ NK cells), showing significantly greater number of CD3$^{+}$ T and CD8$^{+}$ T cells in range to CD3$^{+}$ T center cells than to NKp46$^{+}$ NK cells. (C) Number of CD3$^{+}$ T, CD8$^{+}$ T, and NKp46$^{+}$ NK cells in 30μm radius to NKp46$^{+}$ NK center cells, showing significant clustering of NKp46$^{+}$ NK with other NKp46$^{+}$ NK compared to T cells. ****, P<0.0001.

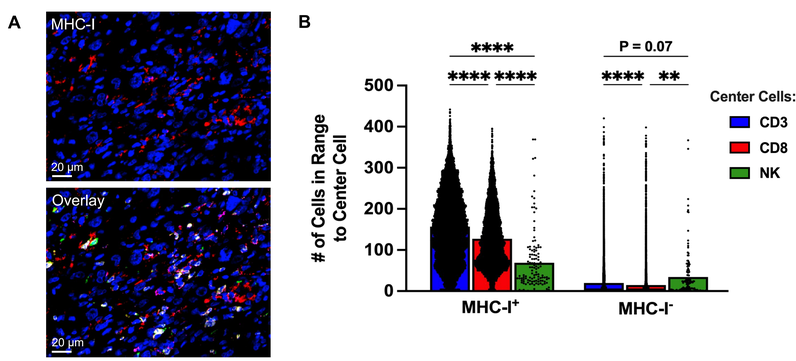


**Figure 9.** (A) Representative immunofluorescence photomicrographs of MHC-I and overlay with CD3, CD8, and NKp46. (B) Number of CD3$^{+}$ T, CD8$^{+}$ T, and NKp46$^{+}$ NK cells in 30μm radius to MHC-I$^{+}$ and MHC-I$^{-}$ cells. **, P<0.01; ****, P<0.0001.